ACS MATERIALS LETTERS

www.acsmaterialsletters.org

Ultrafast Joule Heating Processing of Lunar Soil Minerals for Water Electrolysis

Yuan Zhong,[‡] Yuanhao Liu,[‡] Zehua Liu, Xuecheng Guo, Yawen Jiang, Chao Zhang, Lin Zu, Yuan Zhao, Li−Li Ling, Ran Long,* and Yujie Xiong*

Cite This: *ACS Materials Lett.* 2025, 7, 553−559

Read Online

ACCESS | Metrics & More | Article Recommendations | Supporting Information

ABSTRACT: Maximizing the utilization of *in situ* extraterrestrial resources, including solar-powered water electrolysis using lunar soil as a catalyst, is a promising strategy for achieving a sustainable fuel and oxygen supply for lunar exploration. However, these lunar soil-based silicate minerals suffer from unsatisfactory intrinsic activity for water splitting due to poor electrical conductivity and the lack of catalytic sites. Here we report the use of a simple Joule-heating method to sinter the minerals into a disordered matrix at ∼2000 °C. The as-prepared amorphous minerals can significantly reduce the overpotential and exhibit good stability (>150 h) due to enhanced charge transport kinetics and intrinsic activity. We further demonstrate the solar-driven water electrolysis stack using sintered lunar soil simulants as catalysts, showing the practicality of such a system. This work provides insights into *in situ* resource utilization of lunar soils by engineering crystalline structures and electronic configurations by using an ultrafast Joule-heating method.

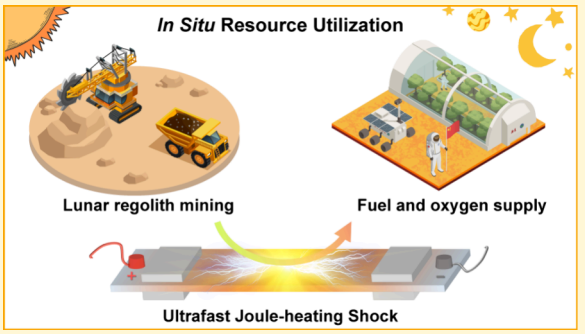

Space colonization has been a perennial human dream,[1,2] and the Moon is intended to be a stepping stone in the exploration march.[3] In order to fulfill this fanciful dream, one of the most important prerequisites is the establishment of a life support system on the Moon.[4] However, current extraterrestrial survival is largely dependent on Earth-based resources, including fuel and oxygen for human energy and breathing needs, which takes up the limited payload of spacecraft and increases the launch costs.[5] *In situ* resource utilization (ISRU) is the use of local natural resources (e.g., solar radiation, water ice, and planetary regolith) at extraterrestrial sites to produce products and services for space exploration.[4,6,7] Given the abundance of regolith and the possible existence of water ice on the Moon,[5,8,9] solar-powered water electrolysis using lunar soil as an electrocatalyst has attracted intense interest as an important part of ISRU.[3,4,10]

However, the accessibility of efficient catalysts is a major obstacle to extraterrestrial water electrolysis. Compared to the well-developed electrocatalysts on Earth,[11] lunar soil or its components (mainly silicate minerals) usually suffer from high overpotential for water decomposition due to the poor electrical conductivity and lack of catalytic active sites.[3,12,13] Recently, the ultrafast Joule heating shock has emerged as a promising method due to its unique ability to modulate the crystal and electronic structures to enhance the charge transfer kinetics and intrinsic activity of catalysts, such as single-atom catalysts,[14] cermets,[15] high-entropy alloys,[16] and metallic glass nanoparticles.[17] In this method, samples loaded on a conductive substrate are subjected to current pulses in a vacuum or inert atmosphere, undergoing hypervelocity heating by the electrical energy ($Q = I^2Rt$) and rapid cooling to room temperature.[18] In particular, the simple device and transient heating characteristics make this method suitable for automated operation in extreme space environments (e.g., microgravity, temperatures ranging from −171 to 140 °C, and high vacuum on the Moon).[19]

In this regard, it is conceivable to screen the active components in lunar soils and treat the minerals using the Joule heating method for efficient water decomposition. Here, we evaluated the hydrogen evolution reaction (HER) performance of lunar soil simulants and known mineral components (including plagioclase, augite, olivine, and ilmenite), in which augite showed relatively better HER activity with an overpotential of 641.5 mV in 0.5 M H_2SO_4 at a current density of 10 mA cm^{-2}. Furthermore, we used the Joule heating method to sinter augite into an amorphous matrix at 2000 °C in seconds,

Received: December 1, 2024
Revised: January 4, 2025
Accepted: January 7, 2025

https://doi.org/10.1021/acsmaterialslett.4c02448
ACS Materials Lett. 2025, 7, 553−559

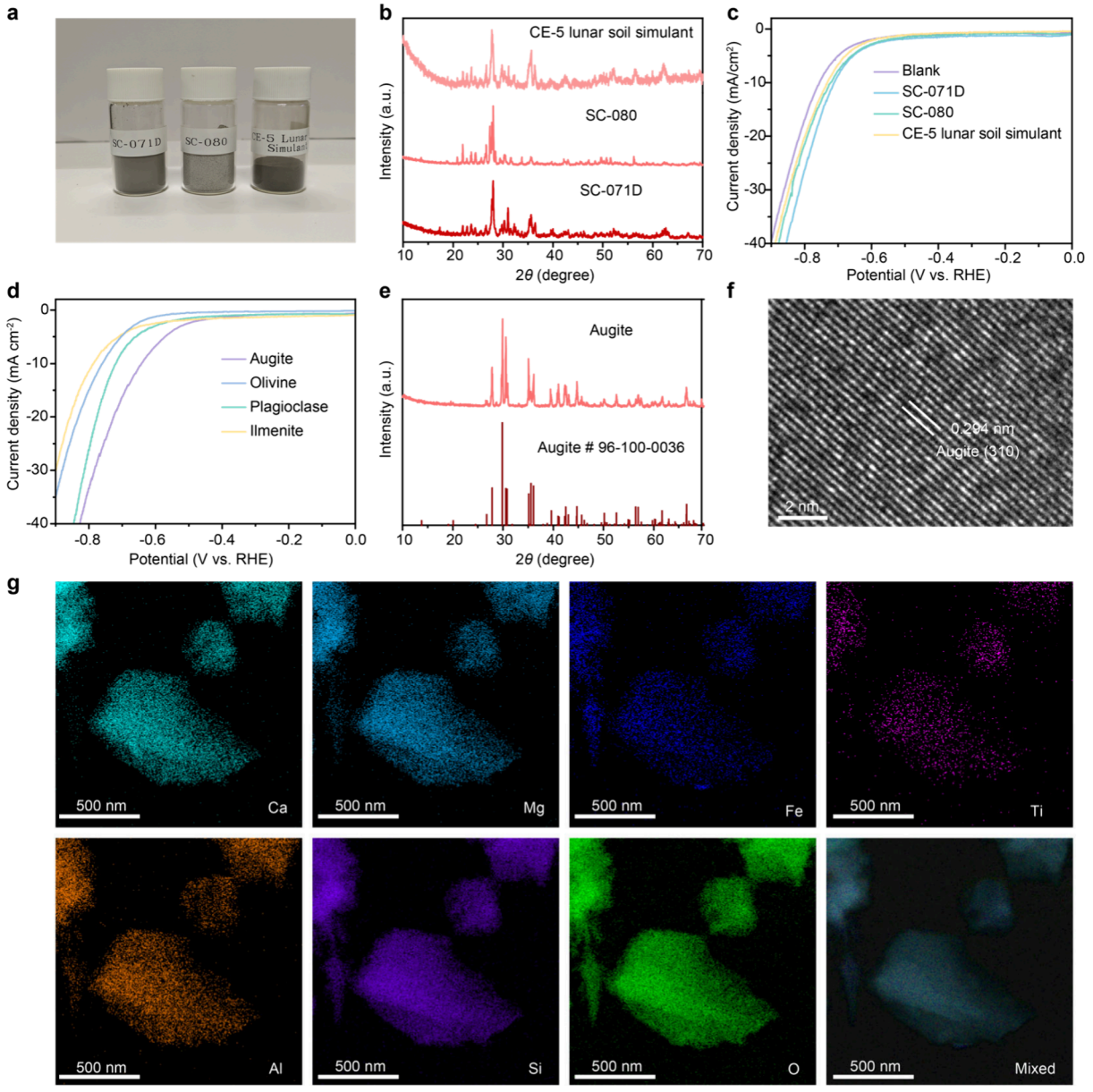

Figure 1. (a) Photograph of SC-071D, SC-080, and CE-5 lunar soil simulants. (b) XRD patterns of the lunar soil simulants. (c−d) LSV curves of lunar soil simulants (c) and the containing mineral components (d). All the potentials were reported without *iR* compensation. (e−g) XRD patterns (e), HRTEM image (f), and EDS elemental mapping profiles (g) of augite.

which exhibited drastically improved HER performance (389.0 mV at 10 mA cm^{-2} for HER overpotential) and good stability due to better charge transport kinetics and intrinsic activity. To avoid tedious mineral separations, lunar soil simulants were also directly sintered to provide efficient and stable catalysts that maintain a low overpotential for 150 h. In addition, we assembled an electrolyzer stack for splitting pure water using the sintered Chang'E-5 lunar soil simulant (referred to as CE-5) as the catalyst and used a photovoltaic cell to harvest solar energy and power the electrolysis module. The system achieved sustained production of hydrogen (~7.54 mL/min) and oxygen (~3.77 mL/min), demonstrating the high practicality of ISRU in outer space.

HER PERFORMANCE OF THE SILICATE MINERALS

Lunar regolith, usually containing rock chips, mineral fragments, glass, and breccias, was created through space weathering and meteorite impacts.[5,20] To date, humans have launched hundreds of lunar exploration spacecraft, and completed 11 lunar sample return missions (i.e., 6 Apollo missions, 3 Luna-series space probes, and 2 Chang'E landers),[10] obtaining a total weight of 385.67 kg of lunar samples.[21,22] Considering the rather precious nature of lunar soil, we used lunar regolith simulants (SC-071D and SC-080) as substitutes in this work (Figures 1a,b and S1), whose composition and particle size distribution matched those of typical Apollo samples.[23] Specifically, SC-071D (akin to the regolith on the lunar plain) is a mixture of augite (32.8 wt %), plagioclase (19.8 wt %), olivine (11.1 wt %), and ilmenite (4.3 wt %), while SC-080 is mainly composed of plagioclase (74.4 wt %), simulating the lunar plateau soils. In addition, according to the known composition,[3] we also obtained the simulant of CE-5 lunar soil, which is mare basalt mined from the Northern Oceanus Procellarum basin on the Moon.[24]

https://doi.org/10.1021/acsmaterialslett.4c02448
ACS Materials Lett. 2025, 7, 553−559

We first evaluated the electrochemical hydrogen evolution reaction (HER) performance of the lunar regolith simulants using a three-electrode system in 0.5 M H_2SO_4. The standard potential of the reference electrode was calibrated under the same conditions before the electrochemical test (Figure S2), and a graphite rod was used as the anode to avoid any potential contamination.[25] For comparison, we also tested the HER performance of the bare glass carbon. As illustrated in Figure 1c, lunar soil simulants could promote HER compared to glass carbon, while the SC-071D simulant had a lower overpotential (712.5 mV@10 mA cm^{-2}) for HER. To screen the active component, we investigated the electrocatalytic performance of different mineral compositions of the simulants separately (Figures S3−S7). Augite, one of the most common rock-forming minerals throughout Earth, the Moon, and Mars,[26] demonstrated the superior catalytic activity (641.5 mV@10 mA cm^{-2}) among these minerals (Figure 1d). Notably, the augite sample in this work had good crystallinity (Figure 1e), and the high-resolution transmission electron microscopy (HRTEM) image displayed distinct lattice fringes with an interplanar space of 0.294 nm, consistent with the (310) plane of augite (Figure 1f). The energy-dispersive X-ray spectroscopy (EDS) mapping images indicated a uniform distribution of element compositions, including Ca, Mg, Fe, Ti, Al, Si, and O (Figure 1g).

Although augite can promote HER, the overpotentials of the silicate minerals remain too high for practical applications, leading to substantial energy consumption. Thus, the continual reduction of overpotential is vital for ISRU of lunar soil as an electrocatalyst for water splitting. Considering the composition and structure of the lunar soil-based minerals, the low HER activity could be attributed to the poor charge transfer kinetics and lack of catalytic sites.[13] In this regard, it is highly desired to develop a methodology for optimizing minerals by endowing more active sites and better electrical conductivity. In addition, the methodology should be simple and feasible for operating the system in a lunar environment.

MINERALS SINTERING VIA THE JOULE HEATING METHOD

The Joule heating method can utilize millisecond current pulses to achieve rapid heating and quenching (Figure 2a).[27] The simplicity of the device and its transient heating characteristics make it suitable for high-throughput synthesis of functional materials in extraterrestrial sites.[18] Therefore, we chose augite as the representative lunar soil-based mineral and employed an ultrafast flash Joule heating method to sinter it (denoted as augite-JX, where X represents the sintering temperature). In a typical procedure, augite was placed onto a tungsten boat and sintered for 2 s at 2000 °C, followed by rapid cooling (Figures 2b,c, and S8). To investigate the detailed sintering process and the evolution of the microstructure, we tuned the processing temperatures (1000, 1500, and 2000 °C) following the same procedure. After flash Joule heating shock, the augite powder was transformed into a pellet, and its size was significantly reduced (Figure 2c), indicating that the bulk augite was melted and crushed during the process. Interestingly, the crystallinity of augite decreased dramatically with an increase in sintering temperature (Figure 2d). When the temperature was up to 2000 °C, the X-ray diffraction (XRD) pattern did not show any peaks from crystalline compositions, except for the broad diffraction peaks from the amorphous matrix. The disordered structure was further confirmed by HRTEM and the corresponding fast Fourier transformation (FFT) pattern (Figure 2e), where the

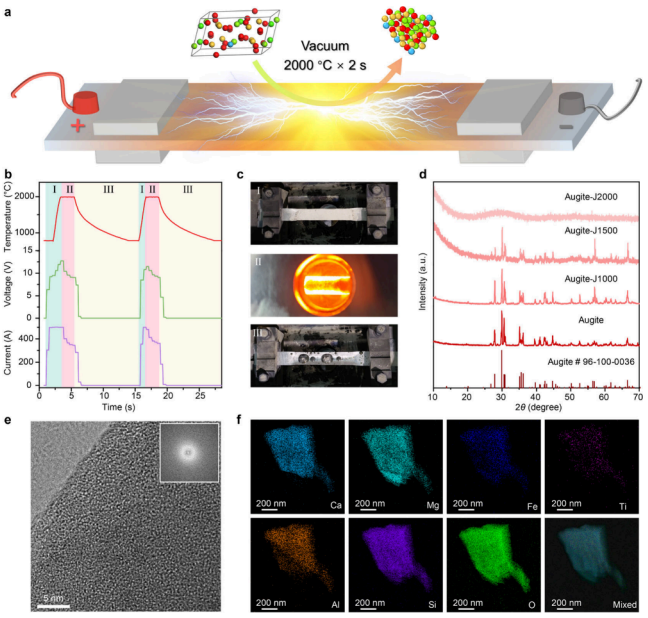

Figure 2. (a) The schematic illustration of sintering lunar soil-based minerals with the ultrafast Joule heating method. (b) The temperature, applied current, and voltage during the process. (c) The optical images of the Joule heating system. (d) XRD patterns of augite and augite-JX. (e) HRTEM image of an augite-J2000. The inset of (e) shows the fast Fourier transform pattern. (f) EDS elemental mapping images of augite-J2000 for Ca, Mg, Fe, Ti, Al, Si, and O.

lattice fringes disappeared after a high-temperature shock. The elemental mapping images exhibited a homogeneous distribution of Ca, Mg, Fe, Ti, Al, Si, and O in the augite-J2000 catalyst (Figure 2f), akin to that of augite before sintering (Figure 1g). These results jointly indicated that augite-J2000 turned into an amorphous and uniform matrix. Indeed, the glass transition due to the rapid heating and quenching process is very common in solid-state physics and metallurgy.[28,29] During the Joule-heating process, the silicate minerals melted and quenched so rapidly that the internal atoms were frozen near the position where they were in the liquid state before they could crystallize and nucleate, thus forming the amorphous glass phase. Notably, these elements with valence less than 4 in augite (such as Ca, Mg, Al, etc.) helped to break up the Si−O tetrahedron network structure,[30] resulting in numerous lattice defects, e.g., 3-fold- and 5-fold-coordinated atoms. According to previous reports, the long-range disordered structure could be beneficial for catalytic application due to more dangling bonds and abundant defects on its surface than its crystallized counterparts.[31] We further used X-ray photoemission spectroscopy (XPS) to investigate the electronic structures of augite and augite-J2000. In the high-resolution XPS spectrum of augite, the Ti 2p peak was split into two peaks of Ti $2p_{3/2}$ and $2p_{1/2}$ (Figure S9a), and the Ti $2p_{3/2}$ peak at 459.10 eV was assigned to Ti^{4+} in Ti−O. After the ultrafast Joule heating shock, the Ti $2p_{3/2}$ spectrum of augite-J2000 showed a negative shift of binding energy by ∼0.52 eV relative to that of augite (Figure 3a), indicating the changed chemical environment of Ti. We further performed peak fitting and deconvolution. Notably, the Ti 2p spectrum of augite-J2000 displayed a characteristic Ti−O−Fe^{2+} peak at 458.48 eV.[32] A similar shift toward lower binding energy was also observed in the high-resolution Fe 2p XPS spectra, suggesting the decreasing valence state of Fe in augite-J2000 (Figures 3b and S9b). The Fe

https://doi.org/10.1021/acsmaterialslett.4c02448
ACS Materials Lett. 2025, 7, 553−559

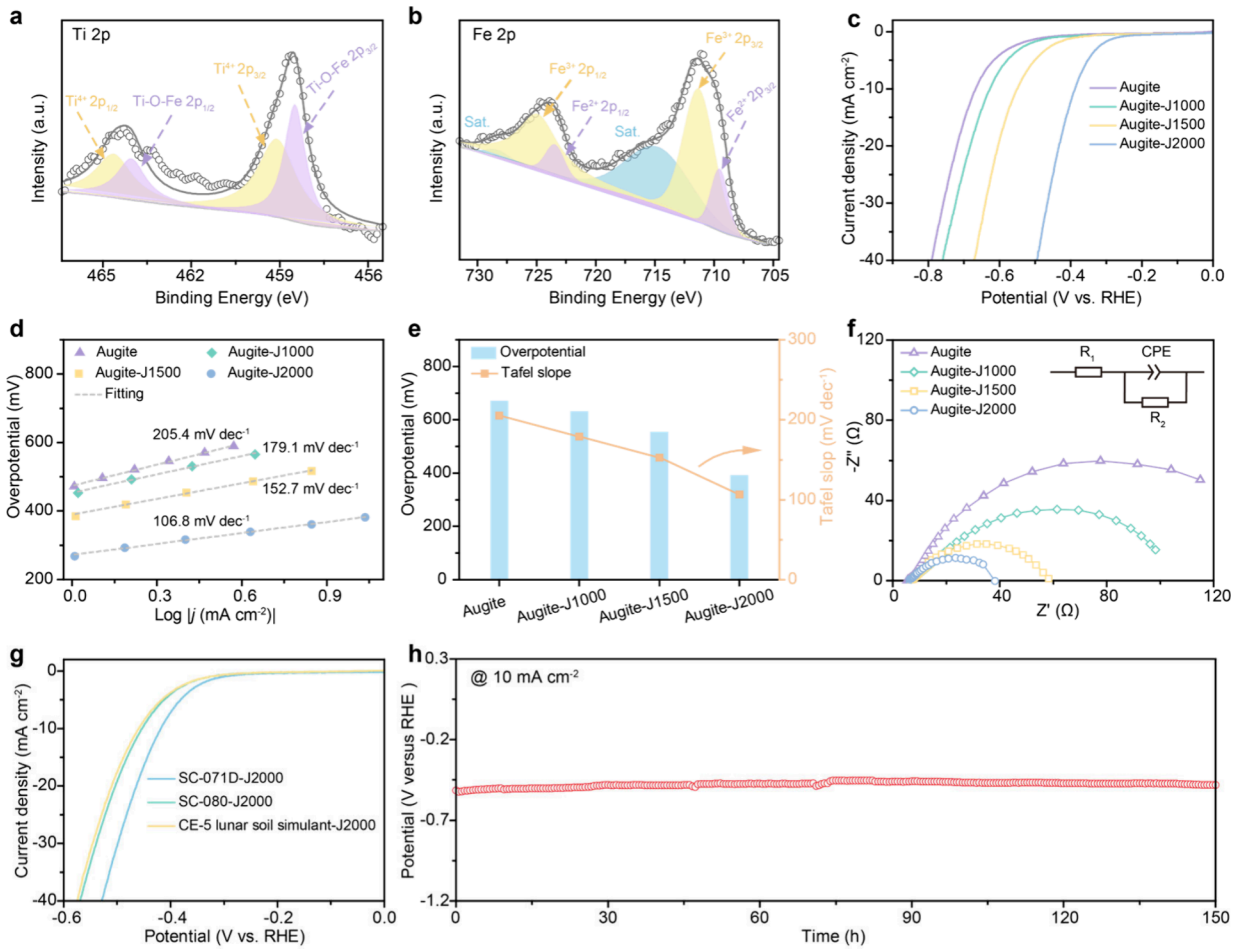

Figure 3. (a–b) High-resolution XPS spectra of Ti 2p (a) and Fe 2p (b) for augite-J2000. (c–d) LSV polarization curves (c) and the corresponding Tafel plots (d) of augite and augite-JX in 0.5 M H_2SO_4. (e) Comparison of overpotentials at a current density of 10 mA cm^{-2} and Tafel slopes for augite and augite-JX. (f) The Nyquist plots of augite and augite-JX. The equivalent circuit diagram was depicted in the inset of (f). R_1: the solution resistance; CPE: the constant phase element; R_2: the charge-transfer resistance.[25] (g) LSV polarization curves of the lunar soil simulants after the Joule heating shock under 2000 °C. (h) Stability measurement of CE-5 lunar soil simulant-J2000 at a current density of 10 mA cm^{-2}. All the potentials were reported without *iR* compensation.

$2p_{3/2}$ peak at 711.30 eV was assigned to Fe^{3+} (Figure 3b),[33] and a new peak corresponding to Fe^{2+} was found at 709.53 eV,[33] verifying the formation of Ti−O−Fe^{2+}. The reduction of the valence state and the appearance of new chemical bonds could result from ultrahigh-temperature decomposition and bonding during the flash sintering process, which may also promote its electrochemical properties.

ELECTROCHEMICAL PERFORMANCE OF THE SINTERED MINERALS

The electrochemical HER performances of augite sintered at different temperatures (i.e., 1000, 1500, and 2000 °C) were also evaluated in 0.5 M H_2SO_4 (Figure 3c). Significantly, the Joule heating sintered minerals (augite-JX) exhibited boosted HER activity with the increasing temperatures, and the augite-J2000 displayed the lowest overpotential of 389.0 mV at 10 mA cm^{-2}. The corresponding Tafel slope could be calculated from the linear sweep voltammetry (LSV) curve (Figure 3d), which reflected the reaction kinetics.[34] Augite-J2000 showed the least Tafel slope (106.8 mV dec^{-1}) among these samples (Figure 3e), suggesting that the HER proceeded through the Volmer-Heyrovsky mechanism with the electrochemical desorption process as the rate-limiting step.[11] In comparison, the higher Tafel slope of augite (205.4 mV dec^{-1}) indicated inferior HER intrinsic catalytic activity. Furthermore, electrochemical impedance spectroscopy (EIS) analysis was also used to study the reaction kinetics (Figure 3f). The Nyquist plot demonstrated that augite-J2000 had the smallest semicircle radius, revealing that the sintered sample had lower charge transfer resistances and faster hydrogen evolution kinetics. The N_2 adsorption and desorption isotherms showed that augite and augite-J2000 had similar special surface areas (Figure S10). We also estimated the electrochemically active surface area (ECSA) of augite and augite-J2000 by measuring the capacitive current in the nonfaradaic potential region associated with the scan-rate dependence of the cyclic voltammetry.[35] According to the double-layer capacitance (18.18 mF cm^{-2} and 21.75 mF cm^{-2} for augite and augite-J2000, respectively, Figure S11), augite-J2000 (543.75 cm^2) had a larger ECSA than that of augite (454.50 cm^2). The geometric current density was further normalized by the measured ECSA to exclude the influence of the surface area on HER performance (Figure S12). Impressively, augite-J2000 showed a significantly higher normalized current density than the counterpart of augite, reflecting the enhanced intrinsic HER activity after the Joule heating process.

https://doi.org/10.1021/acsmaterialslett.4c02448
ACS Materials Lett. 2025, 7, 553−559

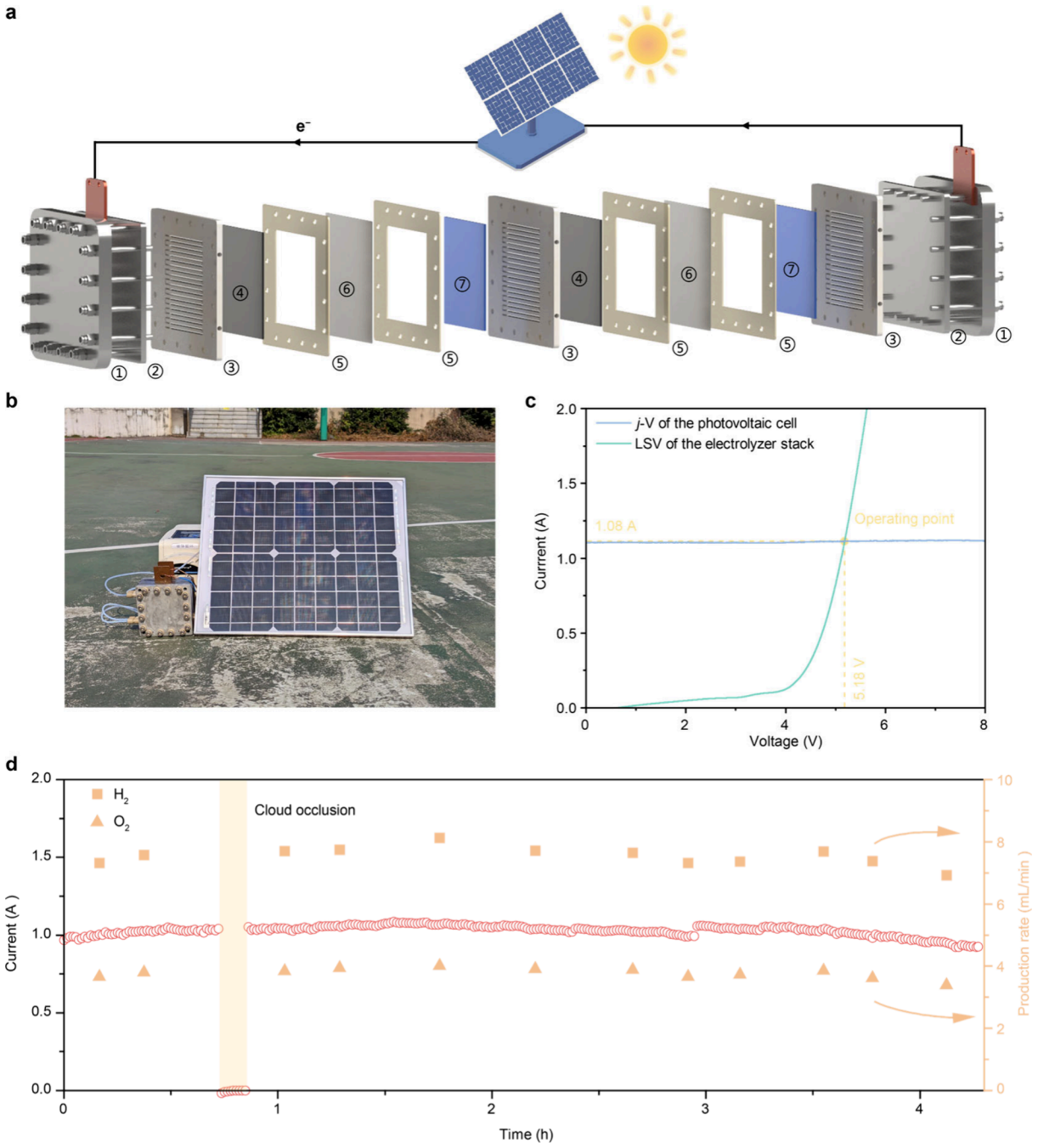

Figure 4. (a) Schematic illustration of water electrolysis in an electrolyzer stack, powered by a photovoltaic cell. ①: end plate. ②: current collector. ③: flow field. ④: cathode. ⑤: sealing gasket. ⑥: proton-exchange membrane. ⑦: anode. (b) The photograph of solar-driven water electrolysis in an electrolyzer stack with CE-5 lunar soil simulant-J2000 as the catalyst. (c) Photovoltaic and electrocatalytic *J*-V behaviors. The *J*-V curve of the solar cell (blue line) was measured under solar irradiation with a light intensity of 68 mW cm^{-2}. The orange dot is the intersection of the *J*-V curve of the solar cell and the LSV curve (cyan line) of the electrolyzer stack, representing the operating point. (d) Stable hydrogen and oxygen production demonstration of the electrochemical system powered by a photovoltaic cell.

In addition, augite-J2000 demonstrated negligible HER activity attenuation during a constant-current electrolysis test at 10 mA cm^{-2} for 95 h (Figure S13). After the stability test, the morphology and amorphous structure were retained (Figure S14 and S15), and the elemental mapping still showed a uniform distribution of Ca, Mg, Fe, Ti, Al, Si, and O without element aggregation in the post-HER sample (Figure S16). Hence, the above performance evaluation and spectroscopic results verified that the ultrafast Joule heating method could optimize lunar soil-based minerals and promote their intrinsic activity and charge transport capability by regulating the crystal and electronic structures. It is worth noting that the simplicity of the device and its tolerance to extraterrestrial environments would make the method a promising alternative for ISRU of abundant planetary regolith.

As a proof of concept, we sintered lunar soil simulants directly through a Joule heating shock to avoid tedious mineral separation. These simulants after the high-temperature (2000 °C) process also turned into a disordered matrix according to the corresponding XRD patterns (Figure S17). In addition, no

https://doi.org/10.1021/acsmaterialslett.4c02448
ACS Materials Lett. 2025, 7, 553−559

distinct morphology difference was observed in these samples before and after sintering (Figure S1 and S18). Interestingly, these sintered soils showed similar HER performance (419.0, 454.0, and 460.0 mV at 10 mA cm^{-2} for SC-071D-J2000, SC-080D-J2000, and CE-5 lunar soil simulant-J2000, respectively) (Figure 3g). The CE-5 lunar soil simulant-J2000 catalyst also achieved good retention of the applied potential during a 150 h constant current stability test (Figure 3h). The universality of this method means that it can act as a potentially powerful tool for ISRU of lunar soil at random landing sites on the Moon. To further demonstrate the high practicality of such a system at extraterrestrial sites, we assembled an electrolyzer stack and used a photovoltaic cell to perform solar-driven water electrolysis (Figures 4a,b, and S19). In the electrochemical module, we used CE-5 lunar soil simulant-J2000 as the catalyst, and pure water was directly adopted for electrolysis. On a sunny day (23 November 2024, 68 mW cm^{-2}) in Hefei (31°49′14″N, 117°13′38″E), the photovoltaic cell obtained an open-circuit voltage of 23.40 V and a short-circuit current of 1.10 A. When integrating the solar cell with the electrolyzer stack, the system achieved stable hydrogen (∼7.54 mL/min) and oxygen (∼3.77 mL/min) production at a voltage of ∼5.18 V and a current of ∼1.08 A (Figure 4c,d). Obviously, the sustained supply of fuel and oxygen in such a system enables the maximum utilization of extraterrestrial resources, including rich solar irradiation and regolith, demonstrating the attractive perspective of ISRU.

In summary, lunar soil acting as the electrocatalyst of water decomposition is a promising strategy for a sustainable fuel and oxygen supply on the Moon. In this work, we identified the active components (i.e., augite) for HER and provided an effective strategy to tune the crystalline structures and electronic configurations of the minerals with the ultrafast Joule heating method. Benefiting from enhanced intrinsic activity and charge transport kinetics, the obtained amorphous minerals exhibited a drastically improved HER performance, achieving an overpotential of 389.0 mV at a current density of 10 mA cm^{-2} and impressive stability (>150 h). An electrolyzer stack powered by a photovoltaic cell was also assembled for stable hydrogen and oxygen production using sintered CE-5 lunar soil simulants as catalysts. This work demonstrates the feasibility of the Joule heating method to optimize the catalytic properties of lunar soil and provides insight into the ISRU of planetary regolith.

■ ASSOCIATED CONTENT

Supporting Information

The Supporting Information is available free of charge at https://pubs.acs.org/doi/10.1021/acsmaterialslett.4c02448.

Detailed experimental procedures, characterization methods, and supporting figures (PDF)

■ AUTHOR INFORMATION

Corresponding Authors

Ran Long − *Hefei National Research Center for Physical Sciences at the Microscale, School of Chemistry and Materials Science, and National Synchrotron Radiation Laboratory, University of Science and Technology of China, Hefei, Anhui 230026, China;* orcid.org/0000-0003-4845-9120; Email: longran@ustc.edu.cn

Yujie Xiong − *Hefei National Research Center for Physical Sciences at the Microscale, School of Chemistry and Materials Science, and National Synchrotron Radiation Laboratory, University of Science and Technology of China, Hefei, Anhui 230026, China; Suzhou Institute for Advanced Research, University of Science and Technology of China, Suzhou, Jiangsu 215123, China; Anhui Engineering Research Center of Carbon Neutrality, The Key Laboratory of Functional Molecular Solids, Ministry of Education, College of Chemistry and Materials Science, Anhui Normal University, Wuhu, Anhui 241002, China;* orcid.org/0000-0002-1995-8257; Email: yjxiong@ustc.edu.cn

Authors

Yuan Zhong − *Hefei National Research Center for Physical Sciences at the Microscale, School of Chemistry and Materials Science, and National Synchrotron Radiation Laboratory, University of Science and Technology of China, Hefei, Anhui 230026, China*

Yuanhao Liu − *Hefei National Research Center for Physical Sciences at the Microscale, School of Chemistry and Materials Science, and National Synchrotron Radiation Laboratory, University of Science and Technology of China, Hefei, Anhui 230026, China*

Zehua Liu − *Hefei National Research Center for Physical Sciences at the Microscale, School of Chemistry and Materials Science, and National Synchrotron Radiation Laboratory, University of Science and Technology of China, Hefei, Anhui 230026, China*

Xuecheng Guo − *Hefei National Research Center for Physical Sciences at the Microscale, School of Chemistry and Materials Science, and National Synchrotron Radiation Laboratory, University of Science and Technology of China, Hefei, Anhui 230026, China*

Yawen Jiang − *National Key Laboratory of Deep Space Exploration, Hefei, Anhui 230000, China*

Chao Zhang − *Hefei National Research Center for Physical Sciences at the Microscale, School of Chemistry and Materials Science, and National Synchrotron Radiation Laboratory, University of Science and Technology of China, Hefei, Anhui 230026, China*

Lin Zu − *National Key Laboratory of Deep Space Exploration, Hefei, Anhui 230000, China*

Yuan Zhao − *National Key Laboratory of Deep Space Exploration, Hefei, Anhui 230000, China*

Li−Li Ling − *National Key Laboratory of Deep Space Exploration, Hefei, Anhui 230000, China*

Complete contact information is available at: https://pubs.acs.org/10.1021/acsmaterialslett.4c02448

Author Contributions

‡Y.Z. and Y.L. contributed to this work equally. All authors have approved the final version of the manuscript.

Notes

The authors declare no competing financial interest.

■ ACKNOWLEDGMENTS

This work was financially supported by the National Major Engineering Key Technology R&D Program, NSFC (U23A2091, 22122506, 22479139, 22232003), Anhui Provincial Natural Science Foundation (2408085JX001), Youth Innovation Promotion Association of CAS (Y2023129), and Fundamental Research Funds for the Central Universities (KY2140000031, WK2060000099). We thank the support from the USTC Center for Micro- and Nanoscale Research and Fabrication and the Instruments Center for Physical Science,

USTC. This work was partially carried out at the Instruments Center for Physical Science, University of Science and Technology of China. Part of the icons in TOC come from macrovector/Freepik.

REFERENCES

(1) Smith, C. M.; Davies, E. T. S. *Emigrating Beyond Earth: Human Adaptation and Space Colonization*; Springer, 2012.
(2) O'Neill, G. K. The Colonization of Space. *Phys. Today* **1974**, *27*, 32−40.
(3) Yao, Y.; Wang, L.; Zhu, X.; Tu, W.; Zhou, Y.; Liu, R.; Sun, J.; Tao, B.; Wang, C.; Yu, X.; et al. Extraterrestrial Photosynthesis by Chang'E-5 Lunar Soil. *Joule* **2022**, *6*, 1008−1014.
(4) Yang, L.; Zhang, C.; Yu, X.; Yao, Y.; Li, Z.; Wu, C.; Yao, W.; Zou, Z. Extraterrestrial Artificial Photosynthetic Materials for *in-situ* Resource Utilization. *Natl. Sci. Rev.* **2021**, *8*, nwab104.
(5) Sanders, G. B.; Larson, W. E. Progress Made in Lunar *in situ* Resource Utilization under NASA's Exploration Technology and Development Program. *J. Aerosp Eng.* **2013**, *26*, 5−17.
(6) Anand, M.; Crawford, I. A.; Balat-Pichelin, M.; Abanades, S.; van Westrenen, W.; Péraudeau, G.; Jaumann, R.; Seboldt, W. A Brief Review of Chemical and Mineralogical Resources on the Moon and Likely Initial *in situ* Resource Utilization (ISRU) Applications. *Planet. Space Sci.* **2012**, *74*, 42−48.
(7) Starr, S. O.; Muscatello, A. C. Mars *in situ* Resource Utilization: A Review. *Planet. Space Sci.* **2020**, *182*, 104824.
(8) Song, H.; Zhang, J.; Ni, D.; Sun, Y.; Zheng, Y.; Kou, J.; Zhang, X.; Li, Z. Investigation on *in-situ* Water Ice Recovery Considering Energy Efficiency at the Lunar South Pole. *Appl. Energy* **2021**, *298*, 117136.
(9) Li, S.; Lucey, P. G.; Milliken, R. E.; Hayne, P. O.; Fisher, E.; Williams, J. P.; Hurley, D. M.; Elphic, R. C. Direct Evidence of Surface Exposed Water Ice in the Lunar Polar Regions. *Proc. Natl. Acad. Sci. U.S.A.* **2018**, *115*, 8907−8912.
(10) Zhong, Y.; Low, J.; Zhu, Q.; Jiang, Y.; Yu, X.; Wang, X.; Zhang, F.; Shang, W.; Long, R.; Yao, Y.; Yao, W.; Jiang, J.; Luo, Y.; Wang, W.; Yang, J.; Zou, Z.; Xiong, Y. *In Situ* Resource Utilization of Lunar Soil for Highly Efficient Extraterrestrial Fuel and Oxygen Supply. *Natl. Sci. Rev.* **2023**, *10*, nwac200.
(11) Zhao, G.; Rui, K.; Dou, S. X.; Sun, W. Heterostructures for Electrochemical Hydrogen Evolution Reaction: A Review. *Adv. Funct. Mater.* **2018**, *28*, 1803291.
(12) Papike, J.; Taylor, L.; Simon, S. *Lunar Sourcebook: A User's Guide to the Moon*; Cambridge, 1991.
(13) Wan, H.; Ma, W.; Zhou, K.; Cao, Y.; Liu, X.; Ma, R. Advanced Silicon Nanostructures Derived from Natural Silicate Minerals for Energy Storage and Conversion. *Green Energy Environ.* **2022**, *7*, 205−220.
(14) Xi, D.; Li, J.; Low, J.; Mao, K.; Long, R.; Li, J.; Dai, Z.; Shao, T.; Zhong, Y.; Li, Y.; Li, Z.; Loh, X. J.; Song, L.; Ye, E.; Xiong, Y.; et al. Limiting the Uncoordinated N Species in M-N_x Single-Atom Catalysts toward Electrocatalytic CO_2 Reduction in Broad Voltage Range. *Adv. Mater.* **2022**, *34*, No. e2104090.
(15) Guo, M.; Dong, Q.; Xie, H.; Wang, C.; Zhao, Y.; Wang, X.; Zhong, W.; Li, Z.; Wang, R.; Wang, Y.; et al. Ultrafast High-Temperature Sintering to Avoid Metal Loss toward High-Performance and Scalable Cermets. *Matter* **2022**, *5*, 594−604.
(16) Yao, Y.; Huang, Z.; Xie, P.; Lacey, S. D.; Jacob, R. J.; Xie, H.; Chen, F.; Nie, A.; Pu, T.; Rehwoldt, M.; et al. Carbothermal Shock Synthesis of High-Entropy-Alloy Nanoparticles. *Science* **2018**, *359*, 1489.
(17) Deng, B.; Wang, Z.; Choi, C. H.; Li, G.; Yuan, Z.; Chen, J.; Luong, D. X.; Eddy, L.; Shin, B.; Lathem, A.; Chen, W.; Cheng, Y.; Xu, S.; Liu, Q.; Han, Y.; Yakobson, B. I.; Zhao, Y.; Tour, J. M.; et al. Kinetically Controlled Synthesis of Metallic Glass Nanoparticles with Expanded Composition Space. *Adv. Mater.* **2024**, *36*, No. e2309956.
(18) Yang, W.; Shang, L.; Liu, X.; Zhang, S.; Li, H.; Yan, Z.; Chen, J. Ultrafast Synthesis of Nanocrystalline Spinel Oxides by Joule heating Method. *Chin. Chem. Lett.* **2024**, *35*, 109501.
(19) Schuerger, A. C.; Moores, J. E.; Smith, D. J.; Reitz, G. A Lunar Microbial Survival Model for Predicting the Forward Contamination of the Moon. *Astrobiology* **2019**, *19*, 730−756.
(20) Engelschiøn, V. S.; Eriksson, S. R.; Cowley, A.; Fateri, M.; Meurisse, A.; Kueppers, U.; Sperl, M. EAC-1A: A Novel Large-Volume Lunar Regolith Simulant. *Sci. Rep.* **2020**, *10*, 5473.
(21) Isachenkov, M.; Chugunov, S.; Landsman, Z.; Akhatov, I.; Metke, A.; Tikhonov, A.; Shishkovsky, I. Characterization of Novel Lunar Highland and Mare Simulants for ISRU Research Applications. *Icarus* **2022**, *376*, 114873.
(22) Li, J.; Yin, C.; Chi, S.; Mao, W.; Fu, X.; Zhang, J. The Lunar Regolith Thickness and Stratigraphy of the Chang'E-6 Landing Site. *Remote Sensing* **2024**, *16*, 3976.
(23) Long-Fox, J. M.; Landsman, Z. A.; Easter, P. B.; Millwater, C. A.; Britt, D. T. Geomechanical Properties of Lunar Regolith Simulants LHS-1 and LMS-1. *Adv. Space Res.* **2023**, *71*, 5400−5412.
(24) Qian, Y.; Xiao, L.; Wang, Q.; Head, J. W.; Yang, R.; Kang, Y.; van der Bogert, C. H.; Hiesinger, H.; Lai, X.; Wang, G.; et al. China's Chang'e-5 Landing Site: Geology, Stratigraphy, and Provenance of Materials. *Earth Planet. Sci. Lett.* **2021**, *561*, 116855.
(25) Liu, J.; Wang, D.; Huang, K.; Dong, J.; Liao, J.; Dai, S.; Tang, X.; Yan, M.; Gong, H.; Liu, J.; et al. Iodine-Doping-Induced Electronic Structure Tuning of Atomic Cobalt for Enhanced Hydrogen Evolution Electrocatalysis. *ACS Nano* **2021**, *15*, 18125−18134.
(26) Morrison, S. M.; Downs, R. T.; Blake, D. F.; Prabhu, A.; Eleish, A.; Vaniman, D. T.; Ming, D. W.; Rampe, E. B.; Hazen, R. M.; Achilles, C. N.; et al. Relationships between Unit-Cell Parameters and Composition for Rock-Forming Minerals on Earth, Mars, and Other Extraterrestrial Bodies. *Am. Mineral.* **2018**, *103*, 848−856.
(27) Zhu, L.; Lai, Z.; Xu, J.; Ma, P.; Lu, J.; Xu, Q.; Lin, Y.; Zheng, L.; Wu, L.; Ding, H.; et al. Ultrafast Flash Joule Heating Synthesis of the Pt/MoO_x Heterostructure for Enhancing the Electrocatalytic Hydrogen Evolution Reaction. *J. Mater. Chem. A* **2024**, *12*, 28149−28160.
(28) Manov, V. P.; Popel, S. I.; Buler, P. I.; Manukhin, A. B.; Komlev, D. G. The Influence of Quenching Temperature on the Structure and Properties of Amorphous Alloys. *Mater. Sci. Eng., A* **1991**, *133*, 535−540.
(29) Ishimaru, M.; Munetoh, S.; Motooka, T. Generation of Amorphous Silicon Structures by Rapid Quenching: A Molecular-Dynamics Study. *Phys. Rev. B* **1997**, *56*, 15133−15138.
(30) Jiusti, J.; Zanotto, E. D.; Feller, S. A.; Austin, H. J.; Detar, H. M.; Bishop, I.; Manzani, D.; Nakatsuka, Y.; Watanabe, Y.; Inoue, H. Effect of Network Formers and Modifiers on the Crystallization Resistance of Oxide Glasses. *J. Non-Cryst. Solids* **2020**, *550*, 120359.
(31) Zhang, C.; Hao, X.; Wang, J.; Ding, X.; Zhong, Y.; Jiang, Y.; Wu, M. C.; Long, R.; Gong, W.; Liang, C.; et al. Concentrated Formic Acid from CO_2 Electrolysis for Directly Driving Fuel Cell. *Angew. Chem., Int. Ed. Engl.* **2024**, *63*, No. e202317628.
(32) Meng, Q.; Du, Y.; Yuan, Z.; Xu, Y.; Zhao, X.; Li, L. Study on the Mineral Characteristics and Separation Performances of a Low-TiO_2 Ilmenite. *Miner. Eng.* **2022**, *179*, 107458.
(33) Li, Y.; Huang, F.; Gao, W.; Zhu, Q.; Shen, C.; Li, M.; Sun, X.; Wang, X. Raman Spectroscopy and XPS Study of the Thermal Decomposition of Mg-Hornblende into Augite. *J. Raman Spectrosc.* **2022**, *53*, 820−831.
(34) Shinagawa, T.; Garcia-Esparza, A. T.; Takanabe, K. Insight on Tafel Slopes from a Microkinetic Analysis of Aqueous Electrocatalysis for Energy Conversion. *Sci. Rep* **2015**, *5*, 13801.
(35) Wei, C.; Sun, S.; Mandler, D.; Wang, X.; Qiao, S. Z.; Xu, Z. J. Approaches for Measuring the Surface Areas of Metal Oxide Electrocatalysts for Determining Their Intrinsic Electrocatalytic Activity. *Chem. Soc. Rev.* **2019**, *48*, 2518−2534.

https://doi.org/10.1021/acsmaterialslett.4c02448
ACS Materials Lett. 2025, 7, 553−559